Received: 1 July 2022 | Accepted: 23 November 2022

DOI: 10.1002/ajb2.16115

RESEARCH ARTICLE

American Journal of Botany

Provenance, genotype, and flooding influence growth and resource acquisition characteristics in a clonal, riparian shrub

Emily C. Palmquist[1,2] | **Kiona Ogle**[3] | **Thomas G. Whitham**[2,4] | **Gerard J. Allan**[2,4] | **Patrick B. Shafroth**[5] | **Bradley J. Butterfield**[2]

[1]U.S. Geological Survey, Southwest Biological Science Center, Grand Canyon Monitoring and Research Center, 2255 N Gemini Dr, Flagstaff, AZ 86001, USA

[2]Department of Biological Sciences, Northern Arizona University, Box 5640, Flagstaff, AZ 86011, USA

[3]School of Informatics, Computing and Cyber Systems, Northern Arizona University, Box 5693, Flagstaff, AZ 86011, USA

[4]Center for Adaptable Western Landscapes (CAWL), Northern Arizona University, Box 5640, Flagstaff, AZ 86011, USA

[5]U.S. Geological Survey, Fort Collins Science Center, 2150 Centre Ave., Bldg C, Fort Collins, CO 80526, USA

Correspondence

Emily C. Palmquist, U.S. Geological Survey, Southwest Biological Science Center, Grand Canyon Monitoring and Research Center, 2255 N Gemini Dr, Flagstaff, AZ 86001, USA.
Email: epalmquist@usgs.gov

Abstract

Premise: Riparian plants can exhibit intraspecific phenotypic variability across the landscape related to temperature and flooding gradients. Phenotypes that vary across a climate gradient are often partly genetically determined and may differ in their response to inundation. Changes to inundation patterns across a climate gradient could thus result in site-specific inundation responses. Phenotypic variability is more often studied in riparian trees, yet riparian shrubs are key elements of riparian systems and may differ from trees in phenotypic variability and environmental responses.

Methods: We tested whether individuals of a clonal, riparian shrub, *Pluchea sericea*, collected from provenances spanning a temperature gradient differed in their phenotypes and responses to inundation and to what degree any differences were related to genotype. Plants were subjected to different inundation depths and a subset genotyped. Variables related to growth and resource acquisition were measured and analyzed using hierarchical, multivariate Bayesian linear regressions.

Results: Individuals from different provenances differed in their phenotypes, but not in their response to inundation. Phenotypes were not related to provenance temperature but were partially governed by genotype. Growth was more strongly influenced by inundation, while resource acquisition was more strongly controlled by genotype.

Conclusions: Growth and resource acquisition responses in a clonal, riparian shrub are affected by changes to inundation and plant demographics in unique ways. Shrubs appear to differ from trees in their responses to environmental change. Understanding environmental effects on shrubs separately from those of trees will be a key part of evaluating impacts of environmental change on riparian ecosystems.

KEYWORDS

flooding, genotype, intraspecific variation, multivariate Bayesian mixed effects model, plant physiology, *Pluchea sericea*, provenance, riparian shrub, river flow alteration

Plant species exhibit morphological and physiological variability within and across populations that affects plant performance, which in turn can affect their associated communities and ecosystem properties (Whitham et al., 2012; Evans et al., 2016; Moran et al., 2016; Westerband et al., 2021). Differences in plant phenotypes across the landscape can arise due to phenotypic plasticity, genetic differentiation, local adaptation, and unique combinations of these factors (Whitlock, 2008; Nicotra et al., 2010; Moran et al., 2016; Laitinen and Nikoloski, 2019; Westerband et al., 2021). For riparian plants, intraspecific phenotypic variation can be the result of heritable, genetically based differences related to local adaptation to climate or streamside hydrology (e.g., Evans et al., 2016; Ikeda et al., 2017; Rodríguez et al., 2019; Blasini et al., 2021; Cooper et al., 2022). It can also be related to phenotypic plasticity in response to varying environmental conditions, particularly flooding or air temperature (e.g., Loreti and Oesterheld, 1996; Kozlowski, 2002; Wright et al., 2017; Jeplawy et al., 2021; Lindborg et al., 2021). Phenotypes that vary across a climate gradient could respond uniquely to stream flow alteration (Butterfield et al., 2018, 2020a), leading to unique population responses across a landscape as flow patterns change.

Individuals of riparian plants from provenances (places of origin) that span environmental gradients, such as a temperature gradient, can exhibit adaptive variation in phenology, leaf traits, productivity, and carbon allocation (Grady et al., 2011; Long et al., 2017; Cooper et al., 2019; Blasini et al., 2022). For example, when grown under common conditions, riparian trees from hot provenances can exhibit more conservative leaf traits and different hydraulic strategies—such as lower specific leaf area (SLA), greater leaf conductance, reduced stomatal control, larger root mass, greater sapwood area, and different phenology—than individuals from cooler climates (Grady et al., 2013; Hultine et al., 2020b). These differences are genetically based, related to specific provenance conditions, and persist when grown under new conditions. These provenance-specific phenotypes, then, could have collateral impacts on individual responses to other environmental pressures, such as inundation.

Phenotypic variation in riparian plants is also tied to flooding patterns, such as depth and duration of inundation. Populations can exhibit genetically based, among-population variation in photosynthetic rates, stomatal conductance, root traits, and aboveground morphology under flooded, or inundated, conditions (e.g., Rodríguez et al., 2019; Reents et al., 2021). Inundated plants can also exhibit increases in SLA, decreases in root and total biomass, and photosynthetic changes (Wright et al., 2017; Rodríguez et al., 2019; Reents et al., 2021). Importantly, inundation patterns are changing due to river regulation and climate change (Poff et al., 2007; Perry et al., 2012). Predictions for climate-related flow changes include increased flood risk (Musselman et al., 2018), peak streamflow (Maurer et al., 2018), and annual runoff (Arnell and Gosling, 2013). Additionally, 93% of the world's river volume is predicted to be moderately to severely impacted by dams by 2030 (Grill et al., 2015), which can create flow patterns completely unique from natural flow regimes. Consequently, riparian plant populations have and will likely continue to experience changes to inundation patterns that differ across a species' range and across provenance-specific phenotypes (Nilsson et al., 2005; Capon et al., 2013). Given the clear importance of inundation, local adaptation to temperature, and genetic composition on riparian plant morphology and physiology (e.g., Kozlowski, 1997; De Kort et al., 2014; Garssen et al., 2015; Grady et al., 2015; Long et al., 2017), selection in response to hydrology and inundation may result in local adaptation and ecotype formation (Evans et al., 2016; Ikeda et al., 2017; Cooper et al., 2022). Thus, there is a need to evaluate whether and how variable phenotypes that occur across climate gradients respond to inundation.

Populations of riparian plant species that occur across a broad climate gradient may differentially respond to inundation due to inherent, provenance-based phenotypic differences. Indeed, there is some evidence for trade-offs between phenotypes suited for hot climates and those suited for inundated conditions. For example, habitat suitability modeling suggests that riparian plants can tolerate longer inundation durations in cooler compared to warmer regions (Butterfield et al., 2018). A larger root area to leaf area ratio can be beneficial in hot environments (Hultine et al., 2020a), but root biomass typically decreases when inundated (e.g., Rodríguez et al., 2019; Reents et al., 2021). Further, riparian trees with low SLA can have higher growth rates in hot relative to cool conditions (Grady et al., 2013), but inundated plants can benefit from high SLA due to increased leaf gas diffusion that can compensate for reduced root gas diffusion (Wright et al., 2017). Thus, provenance-specific phenotypes suited for their provenance-specific climate may not align with those suited for inundation, potentially resulting in differential provenance responses to inundation.

We evaluated the influences of provenance, genotype, and inundation on the phenotypic expression of morphological and physiological characteristics of a widespread, woody riparian shrub. While riparian trees are more commonly studied (e.g., Long et al., 2017; González et al., 2018; Hultine et al., 2020b), riparian shrubs can be ecosystem engineers and the dominant overstory plant along many rivers, making their responses a key component of environmental change (e.g., Liljedahl et al., 2020; Butterfield et al., 2020b). We focused on a dominant shrub in the southwestern United States, *Pluchea sericea* (Nutt.) Coville (arrowweed, Asteraceae), collected along the Colorado River in the Grand Canyon, spanning a 5.3°C mean annual temperature gradient. We addressed three hypotheses: (1) In the same environmental conditions, individuals from different provenances will differ in their morphological and physiological phenotypes. Based on studies of the riparian tree, *Populus fremontii* (Hultine et al., 2020b; Blasini et al., 2021), we expected that compared to plants from cooler regions, plants from hotter provenances will have greater photosynthetic rate and stomatal conductance and exhibit traits supporting belowground resource acquisition, such as larger root systems, less aboveground biomass, lower specific leaf area, and lower total leaf area. (2) Individuals from different provenances will differ in their response to inundation. Specifically, individuals from hotter provenances will be more sensitive to inundation; that is, they will have greater decreases in plant productivity, photosynthetic rates, and stomatal conductance when inundated than individuals from cooler provenances. (3) Phenotypic variation in growth and resource acquisition characteristics and inundation responses will be partially governed by genotype. The importance of genotype should be indicated by heritable phenotypic characteristics and inundation responses that are attributable to genotypic variation. When these hypotheses are considered together, if phenotypes and inundation responses are genetically based and differ among plants distributed across a climate gradient, then changes to flow regimes could impact populations differently across a landscape.

MATERIALS AND METHODS

Study species and propagation

We focused on *Pluchea sericea* (arrowweed), a widespread, woody riparian shrub native to dryland rivers of North America (Busch and Smith, 1995). It reproduces sexually and through extensive rhizomes (Vandersande et al., 2001). *Pluchea sericea* is of particular interest in that it often grows in more stressful riparian habitats (e.g., more saline, regulated reaches) than cottonwoods and willows (Busch and Smith, 1995), seems to thrive on regulated rivers, and is impacting recreational resources and riparian geomorphology (Durning et al., 2021). While many native riparian species are in decline in the southwestern United States, *P. sericea* seems to be expanding (Busch and Smith, 1995; González et al., 2020; Durning et al., 2021). It can successfully colonize areas where the abundance of tamarisk (*Tamarix ramosissima*, *Tamarix chinensis*, and hybrids)—nonnative, invasive trees—has been reduced (Busch and Smith, 1995; González et al., 2020).

Collection sites were located along the Colorado River between Glen Canyon Dam and Lake Mead in northern Arizona, United States (Appendix S1, Figure S1). Provenance location is indicated by distance upstream (negative numbers) or downstream (positive numbers) of Lees Ferry, Arizona in kilometers, following regional conventions. Along this 400-km river segment, the elevation drops from 950 m to 366 m a.s.l. resulting in a mean annual temperature increase of about 5.3°C (Caster et al., 2014). Plants were collected in midsummer near five weather stations spanning this temperature gradient (Table 1). Weather data were obtained from Caster et al. (2014) and the NOAA National Centers for Environmental Information Climate Data Online tool (https://www.ncdc.noaa.gov/cdo-web/). A 2-year period when all stations were recording data (2008–2010) was used to estimate nominal site temperatures.

Glen Canyon Dam regulates the Colorado River in the study area, and tributary inputs do not substantially alter flow patterns (Topping et al., 2003), so a similar flow regime exists across the 400-km river segment. Hydropower-derived flows have been in place since 1963 (Topping et al., 2003). *Pluchea sericea* was common in the study area in the pre-dam era (Turner and Karpiscak, 1980) and has increased since river regulation began (Durning et al., 2021). In the study area, this species currently grows above the daily maximum flow volume (708 m^3 s^{-1}, Durning et al., 2021). The five sample sites span a similar shoreline flood gradient and have been flooded for no more than 1 week per year in the last 20 years.

At the end of June and early July 2018, new, nonflowering, cuttings from healthy branches were collected for propagation. At each site, cuttings were collected from across the local stand, which ranged from approximately 1300–2000 m^2 in area. No more than one branch was clipped from one ramet. Each cutting was approximately 30 cm long and 0.3 cm in diameter. Cut ends were wrapped in moist paper towels and stored in plastic bags in coolers. Since documentation for propagating *P. sericea* cuttings was not available, cuttings were initially divided into three equal groups and grown in either pure perlite, a perlite/vermiculite mix, or a mix of perlite, vermiculite, coconut husk, and soil. Twenty cuttings were planted together in 6.5-L pots. Initial propagation methods resulted in similar rates of rooting and survival, so worked equally well. Any mortality almost entirely occurred in this initial propagation step, such that plants that grew roots initially survived until the subsequent greenhouse experiment. Plants were transplanted into individual 6.9 cm diameter × 25.4 cm tubes and grown for another 7 months in a mix of sand, perlite, and vermiculite in a greenhouse. Seven weeks before inundation treatments, plants were transplanted into 36 × 11 × 11 cm (height × length × width) pots. The cuttings were all healthy, well established, and approximately 11 months old at the start of the inundation experiment (below).

TABLE 1 Characteristics of the collection locations (provenances).

Prov.	River km	*N* (Subset)	Genotypes	Temp (°C)	Elev. (m a.s.l.)	Station
1	−4.2	60 (20)	8	17.3, 10.3, 24.3	930	USC00024849, Lees Ferry, AZ
2	91.1	20 (15)	6	19.0, 12.6, 25.4	821	AZ C:13:0365
3	159.0	20 (15)	4	19.4, 12.0, 26.7	686	USC00026471, Phantom Ranch, AZ
4	217.8	90 (20)	1	21.3, 15.0, 27.5	574	AZ B:11:0281
5	354.2	60 (20)	2	22.6, 15.9, 29.4	399	AZ G:03:0072

Notes: Prov., provenance indicator. River km, distance upstream (negative numbers) or downstream (positive numbers) of Lees Ferry, AZ, USA in kilometers; *N* (Subset), full sample size with subset sample size used for "resource acquisition" variables in parentheses; Genotypes, number of multilocus genotypes identified; Temp (°C), mean, minimum, and maximum average temperatures; Elev., elevation in meters; Station, weather station used for climate data.

Inundation design

The experiment exposed 250 *P. sericea* plants to a range of inundation depths inside the climate-controlled Northern Arizona University Research Greenhouse complex in Flagstaff, Arizona. The experiment began on 26 June 2019 and ran for 3 months during the growing season (Appendix S1, Figure S2). Five target inundation depths were predetermined, ranging from the soil and roots being above the water level to the entire pot, all roots, and approximately 15 cm of stem being submerged (Figure 1). The number of replicates for each of the five target inundation depths varied by provenance (Table 1). Ten flooding "systems" were established within the greenhouse, where a "system" comprised five plastic bins connected by tubing and a water pump. Water was circulated through each system with a 2650 L h^{-1} pump. Each bin contained five vertically oriented, 10.2-cm-diameter PVC pipe sections ("tubes"), each cut to one of five heights (49.5, 37.5, 25.5, 13.3, 1.5 cm), to create different levels of inundation. Each tube was filled with sand and one potted plant placed on top (Figure 1). Plants from each provenance were divided equally among the five tube levels and randomized across bins. Roots were able to grow into the water-saturated sand and into the water. The experiment comprised 10 systems, 50 bins, 250 tubes (50 of each height), and 250 individuals.

Each system was filled with water to an established level and refilled to the same level every 2–3 days. Each plant had a unique water level due to differences in pumps and uneven ground. We recorded inundation depth for each plant by measuring the distance between the top of the pot and the water level ("inundation level" hereafter). Negative values indicate an inundated stem (top of the pot below the water level), and positive values indicate a stem out of the water. Inundation level was recorded six times throughout the 3-month study, and the mean for each plant was used as the measure of flooding.

Five temperature sensors were placed inside the greenhouse, so that two systems were represented by one sensor. Air temperature was recorded every 15 min throughout the study. Average greenhouse temperature and humidity were 23°C and 63%, respectively, throughout the study.

Plant measurements

We measured variables related to growth and resource acquisition. Growth variables were measured on all 250

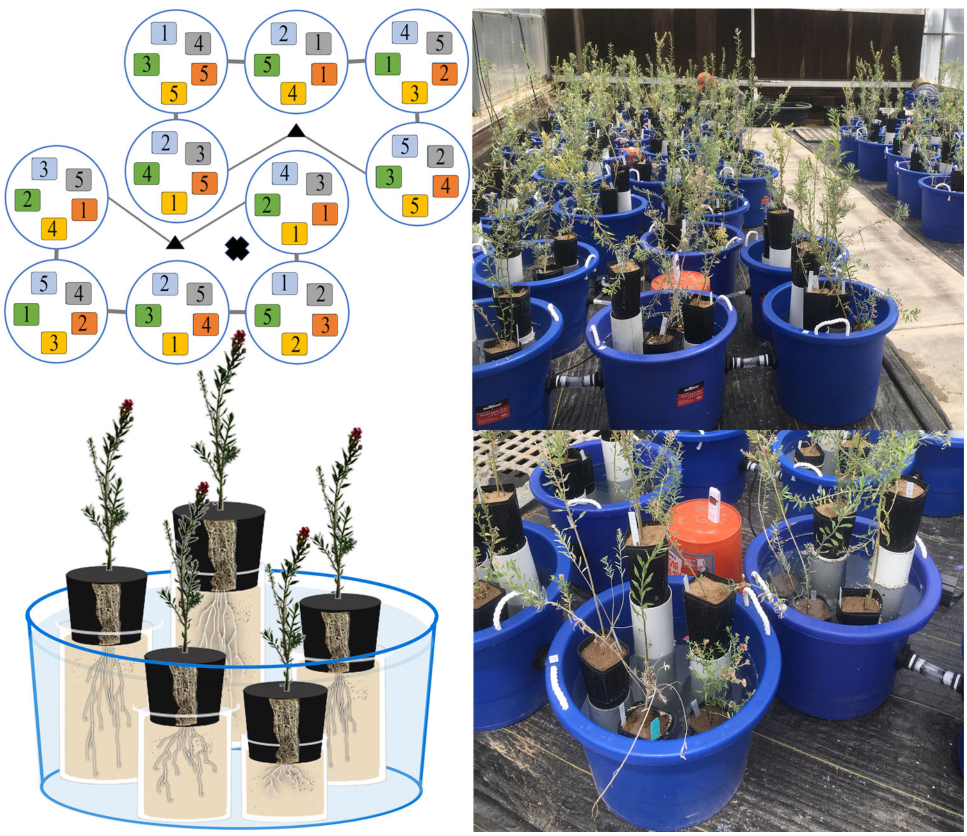

FIGURE 1 Experimental design of flooding system. Upper left panel: A pair of flooding systems is represented. The system consists of five bins connected by tubing and one pump. Black triangles: pumps; circles: plastic bins; ✖: temperature sensor; gray lines: tubes that connect the bins. Colored squares inside the circles represent individual plants, their provenance (number), and their flood treatment (color). Each bin had one each of five heights of PVC tube and a randomized mix of the five provenances. Lower left panel: diagram of one bin containing five individuals in black pots sitting on PVC tubes filled with sand. Roots grew into the water-saturated sand. Right panel: photographs of systems in greenhouse.

individuals and included plant height, stem diameter, average daily growth, final aboveground biomass, and final belowground biomass. Plant height was defined as the height of the tallest living stem. Stem diameter was measured at the soil surface of the single stem. Plant height and stem diameter were measured eight times throughout the study (Appendix S1, Table S1, Figure S3). Average daily growth between each measurement period was calculated as the change in height divided by the number of days between measurements. For analyses, average daily growth was averaged across the last three measurement periods. Aboveground, belowground, and total biomass, and root to shoot biomass ratio were measured or calculated at the end of the experiment (Appendix S1, Table S1). Stems and leaves were clipped, separated into living and dead tissues, and dried. All roots were rinsed and dried. All tissues were dried at 60°C for at least 72 h and until a subset of samples had a consistent weight when weighed 1 day later. Living leaves, living stems, dead leaves, dead stems, and belowground tissues were weighed separately. Aboveground biomass was calculated as the sum of the biomass of living leaves and stems. Belowground biomass represented all coarse and fine roots and the belowground portion of the stem. Total biomass and root to shoot ratio were calculated from above- and belowground biomass measurements.

Resource acquisition variables were measured on a subset of 90 plants representing each provenance and PVC tube height (Table 1). The variables included root length, average root diameter, photosynthetic rate, stomatal conductance, specific leaf area (SLA), and total leaf area (TLA). Root length and diameter were measured before drying at the end of the experiment (Appendix S1, Table S1) with WinRhizo software (Regent Instrument, Quebec City, QC, Canada). Photosynthetic rate (μmol CO_2 m^{-2} s^{-1}) and stomatal conductance (mol H_2O $m^{-2}s^{-1}$) were measured with a LI-6400 XT (LI-COR, Lincoln, NE, USA). Measurements were made in the morning and do not show trends within each sampling morning. Cuvette conditions were maintained at a flow rate of 500 μmol s^{-1}, 420 ppm reference CO_2 concentration, and 1025 μmol m^{-2} s^{-1} photosynthetically active radiation (PAR). Due to small leaf area and short, weak petioles, a fully expanded, young, healthy leaf was removed from the plant and immediately placed in the cuvette. Cuvette conditions were allowed to stabilize (H_2O sample slope < 1, CO_2 sample slope < 1, flow meter slope < 1) before measurements were recorded. Measurements for a single leaf were logged three times within 2 min, leaf area corrected, and averaged to give a single measurement per plant per sampling period. The three measurements during the last month of the experiment were averaged and used in the statistical analyses. At the end of the experiment, SLA (cm^2 g^{-1}) was calculated as fresh leaf area divided by dry leaf mass for 10 healthy, fully expanded, young leaves per plant, and leaf area was calculated using Leafscan (http://www.leafscanapp.com). Leaves were dried at 60°C for 72 h and weighed. The TLA (cm^2) was estimated by multiplying SLA by total leaf biomass. Summary statistics and graphs for these data are presented in Appendix S1, Table S2, Figures S4–S6.

Genetic analyses

We genotyped the subset of 90 individuals used for resource acquisition variables. Leaf samples were dried in silica gel and total genomic DNA was extracted using the protocol developed by Mayjonade et al. (2016) with minor modifications. Seventeen simple sequence repeat (SSR) loci (Yang et al., 2018) were screened for amplification and variability, resulting in three loci that reliably amplified across 90 individuals. An ABI 3730xl Genetic Analyzer (Applied Biosystems, Foster City, CA, USA) was used for fragment analysis with GeneScan LIZ500 internal size standard (ABI). Allele fragment sizes were scored using GeneMarker v2.2.0 (SoftGenetics, State College, PA, USA). Multilocus genotypes (hereafter, "genotypes") were identified using poppr (Kamvar et al., 2014) and R version 3.6.1 (R Core Team, 2014).

Multivariate statistical analyses

Growth and resource acquisition variables were analyzed separately via hierarchical, multivariate Bayesian linear models. The growth model had six response variables: final height (m), average daily growth (mm/day), final stem diameter (cm), final aboveground biomass (g), final belowground biomass (g), and final root to shoot ratio. Total biomass could not be included as an independent variable, as it is a summation of above and belowground biomass. Rather, covariate effects and intercept parameters for total biomass were calculated within the model by adding the corresponding parameters for above- and belowground biomass. Variance parameters and correlations with other variables were not calculated for total biomass. The resource acquisition model included six response variables: the log of final root length (cm), average final root diameter (mm), average photosynthetic rate (μmol CO_2 m^{-2} s^{-1}), average stomatal conductance (mol H_2O m^{-2} s^{-1}), final SLA (cm^2 g^{-1}), and final TLA (cm^2). Two individuals died during the experiment, and some individuals had missing data, resulting in $N = 246$ individuals for the growth model and $N = 89$ individuals for the resource acquisition model.

For each set of variables (growth or resource acquisition), six models were compared (models M1–M6 for growth data, models M7–M12 for resource acquisition data; Tables 2, 3). To evaluate whether response variables differ by provenance, genotype, or both, we compared models that included provenance as a random effect (M1, M7), models that included genotype as a random effect (M2, M8), and models that included both provenance and genotype as random effects (M3, M9). To evaluate whether provenances or genotypes differed in their responses to flooding, the models were modified to allow both intercepts and covariate effects to vary by provenance or genotype, resulting in models M4–M6 and M10-12

TABLE 2 Model fit and DIC values for each growth hierarchical, multivariate Bayesian linear model. Model fit estimates are R^2 values from a linear regression of the individual-level predicted values versus observed values. Model with the lowest DIC is bolded.

Model	Random effects	Covariate effects	DIC	y_1	y_2	y_3	y_4	y_5	y_6	y_7
M1	**Provenance**	No random effect, see Eq. 2	**2204**	**0.33**	**0.23**	**0.22**	**0.31**	**0.30**	**0.16**	**0.33**
M2	Genotype		2242	0.21	0.07	0.28	0.24	0.28	0.18	0.26
M3	Provenance and genotype		2216	0.33	0.24	0.27	0.32	0.34	0.20	0.35
M4	Provenance	Vary by provenance	2218	0.33	0.24	0.26	0.32	0.31	0.17	0.34
M5	Genotype	Vary by genotype	2256	0.21	0.08	0.31	0.24	0.28	0.18	0.26
M6	Provenance and genotype	Vary by provenance	2230	0.33	0.24	0.31	0.32	0.35	0.20	0.35

Notes: Random effects, random effects included in the model in addition to system and bin; Covariate effects, notes whether covariate effects were allowed to vary by provenance or genotype; DIC, deviance information criterion; y_1, final height; y_2, average daily growth; y_3, stem diameter; y_4, aboveground biomass; y_5, belowground biomass; y_6, root:shoot ratio: y_7, total biomass.

TABLE 3 Model fit and DIC values for each resource acquisition hierarchical, multivariate Bayesian linear model. Model fit estimates are R^2 values from a linear regression of the individual-level predicted values versus observed values. Model with the lowest DIC is bolded.

Model	Random effects (Intercept)	Covariate effects	DIC	y_1	y_2	y_3	y_4	y_5	y_6
M7	Provenance	No random effect, see Eq. 2	2076	0.13	0.25	0.64	0.28	0.33	0.35
M8	Genotype		2079	0.16	0.32	0.68	0.30	0.48	0.43
M9	**Provenance and genotype**		**2064**	**0.15**	**0.35**	**0.72**	**0.31**	**0.47**	**0.43**
M10	Provenance	Vary by provenance	2085	0.16	0.31	0.77	0.34	0.39	0.38
M11	Genotype	Vary by genotype	2090	0.30	0.37	0.76	0.38	0.51	0.51
M12	Provenance and genotype	Vary by provenance	2070	0.17	0.39	0.81	0.37	0.52	0.46

Notes: Random effects, random effects included in the model in addition to system and bin; Covariate effects, notes whether covariate effects were allowed to vary by provenance or genotype; DIC, deviance information criterion; y_1, root length; y_2, average root diameter; y_3, photosynthetic rate; y_4, stomatal conductance; y_5, specific leaf area; y_6, total leaf area.

(Tables 2, 3). System and bin were included as random effects in all models, with bins nested in system (Ogle and Barber, 2020). Genotype was not nested in provenance because some genotypes occurred in multiple provenances (Appendix S1, Table S3). Initial models for each response variable that included inundation level, initial plant height, and greenhouse temperature indicated that only inundation level and initial plant height were potentially important predictors of the response variables, including two-way interactions, so only these covariates were used in the multivariate models. All models used standardized covariate values, calculated as $z = (x\text{-mean}[x])/(\text{standard deviation}[x])$, where x = an individual covariate.

The structure of the multivariate models for the growth and resource acquisition variables was identical, apart from a modification to impute unknown genotypes for individuals in the growth model that were not genotyped (described below). The likelihood of the observed vector of response variables, $\mathbf{y}$, for individual i followed the form:

$$\mathbf{y}_i \sim Normal(\boldsymbol{\mu}_i, \Sigma) \tag{1}$$

where $\boldsymbol{\mu}$ is the predicted (or expected) vector value of $\mathbf{y}$, and $\boldsymbol{\Sigma}$ is the 6 × 6 covariance matrix describing the observation variances and covariances among the response variables. Correlations between variables were calculated from the covariance matrix and are presented in Appendix S1, Table S4. The full linear model for $\boldsymbol{\mu}$ that allowed intercepts to vary by provenance and genotype included standardized values of inundation level (z_1) and initial plant height (z_2) as covariates, with provenance ($p = 1, 2, \ldots, 5$), genotype ($g = 1, 2, \ldots, 14$), system ($s = 1, 2, \ldots, 10$ systems), and bin ($b = 1, 2, \ldots, 5$ bins per system) included as random effects is given below, such that for individual i and response variable v:

$$\mu_{i,v} = \beta_{0,v} + \beta_{1,v} z_{1,i} + \beta_{2,v} z_{2,i} + \eta_{p(i),v} + \xi_{g(i),v} + \lambda_{s(i),v} + \varepsilon_{b(i),s(i),v} \tag{2}$$

where subscripts $p(i)$, $g(i)$, $s(i)$, and $b(i)$ denote provenance p, genotype g, system s, and bin b, respectively, associated with individual i. Note that the $z_1 \times z_2$ interaction was not included because prior exploratory analyses indicated that this interaction is not important.

Models M3, M6, M9, and M12 contained all of the random effects in Eq. 2, while the other models contained subsets (Tables 2, 3). Models allowing covariate effects to vary by provenance or genotype in addition to intercepts had the same form, but the coefficient parameters in Eq. 2 ($\beta_{1,v}$ and $\beta_{2,v}$) were additionally indexed by provenance or genotype (e.g., $\beta_{1,v,p(i)}$ and $\beta_{2,v,p(i)}$ or $\beta_{1,v,g(i)}$ and $\beta_{2,v,g(i)}$).

Because the growth model represented all individuals in the experiment, but only a subset was genotyped, growth models including genotype as a random effect (M2, M3, M5, M6) included an additional likelihood to enable imputation of the genotype identity for the nongenotyped individuals. Since the genotype identifier can take on 1 of 14 possibilities, we assumed that the genotype associated with individual i, $g(i)$, can be described by a categorical distribution

$$g\,(i) \sim Categorical\,(\boldsymbol{\theta}_{p\,(i)}) \tag{3}$$

where $\boldsymbol{\theta}_p$ is a vector of length 14 that contains the probabilities of individuals from provenance p being identified as each of the 14 genotypes. A conjugate hierarchical Dirichlet prior was assigned to the provenance-level genotype probabilities, $\boldsymbol{\theta}_p \sim$ Dirichlet($\boldsymbol{\alpha}$), and each component of the $\boldsymbol{\alpha}$ vector was assigned a relatively noninformative exponential prior. The expected probability of a particular genotype, G, for each provenance was calculated from $\boldsymbol{\alpha}$ as

$$p\,(g = G) = \alpha_G / \sum_{g=1}^{14} \alpha_g \tag{4}$$

We also specified zero-centered, hierarchical normal distributions for the random effects in Eq. 2 such that, for example, for the provenance random effects for response variable v, $\eta_{p,v} \sim Normal\,(0, \sigma^2_{\eta,v})$, with similar distributions specified for $\xi_{g,v}$ (genotype random effects), $\lambda_{s,v}$ (system random effects), and $\varepsilon_{b,s,v}$ (bin random effect), each with their own variance term, which is unique to each variable v (e.g., $\sigma^2_{\xi,v}$, $\sigma^2_{\lambda,v}$, $\sigma^2_{\varepsilon,v}$). The associated random effect standard deviations were assigned folded Cauchy distributions that represented relatively non-informative priors (Gelman, 2006). To avoid non-identifiability of the intercept (β_0) and the random effects, we implemented the "post-sweeping of random effects" reparameterization solution as described by Ogle and Barber (2020), with accommodation to nest bins within system. The overall intercept and covariate effects ($\beta_{0,v}$, $\beta_{1,v}$, $\beta_{2,v}$) were assigned conjugate, relatively non-informative normal distributions with a mean of zero and a large variance. For models where the covariate effects varied by provenance or genotype, the effects were assigned hierarchical normal priors centered on an overall effect for that variable; the overall means were assigned relatively non-informative normal distributions and the associated standard deviations were assigned wide uniform, Uniform (0, 150), priors. The precision matrix, $\Omega = \Sigma^{-1}$, in the multivariate likelihoods in Eq. 2 was assigned a relatively non-informative, conjugate Wishart prior. Standard deviations of residuals for each variable were calculated from the covariance matrix.

The above models were implemented in JAGS through the R packages rJAGS (Plummer, 2003; Plummer et al., 2019) and coda (Plummer et al., 2006). Three parallel Markov chain Monte Carlo (MCMC) sequences were assigned broad starting values. The Raftery and Lewis diagnostic (raftery.diag, coda) was used to determine the number of MCMC iterations needed to sufficiently sample the posterior parameters space and chains were thinned. The number of MCMC iterations and the thinning amount varied by model (Appendix S1, Table S5). Convergence, mixing, and autocorrelation were evaluated qualitatively using mcmcplot (mcmcplots; Curtis et al., 2015) and quantitatively using the Gelman and Rubin convergence diagnostic (gelman.diag, coda). Deviance information criterion (DIC) values calculated using the dic.samples function (rJAGS) solely based on the response variables associated with the primary likelihood (Eq. 1) were compared.

Model fit was assessed through simple, linear regression (function lm, base R) of predicted values (posterior means of the individual $\mu_{i,v}$, Eq. 2) on observed values (associated $y_{i,v}$). Posterior distributions of the estimated intercepts and covariate effects were summarized using the posterior means and the 95% central credible intervals (CIs). Significant differences in the additive provenance random effects (e.g., differences in height among provenances) were evaluated by determining whether the 95% CI for a given provenance and variable included zero or not. If the CI for at least one provenance did not contain zero, this provided evidence for a provenance random effect. A similar evaluation was done for the genotype random effects. Likewise, covariate effects are deemed significantly different from zero if their 95% CI does not include zero, meaning that the response variable is likely influenced by the associated covariate (inundation level or initial height).

To estimate heritability of phenotypes, we calculated broad-sense heritability (H^2) using variance parameters estimated for models M3 (growth) and M9 (resource acquisition). Because H^2 is the proportion of phenotypic variance within a population that can be attributed to genetic variability (Visscher, Hill, and Wray, 2008), for each response variable, we estimated H^2 as:

$$H^2 = (\sigma^2_\zeta)/(\sigma^2_\zeta + \sigma^2_\lambda + \sigma^2_\varepsilon + \sigma^2), \tag{5}$$

where σ^2_ζ, σ^2_λ, σ^2_ε and σ^2 denote the genotypic, system, bin, and residual variances, respectively. Both models (M3 and M9) account for provenance and genotypic variance, such that σ^2_ζ is the variance explained by genotype when provenance is also accounted for. H^2 was calculated for each MCMC iteration, allowing posterior summaries of H^2. These estimates of H^2 are representative of heritability under average inundation level and average initial height conditions.

RESULTS

Multilocus genotypes

Fourteen multilocus genotypes were identified and their occurrences varied across provenances (Table 1; Appendix S1, Tables S3, S6). Provenances 1–5 contained 8, 6, 4, 1, and 2 of the 14 genotypes, respectively. The number of individuals per genotype ranged from one to 22.

Provenance phenotypic variability

Hypothesis 1. (under common environmental conditions, individuals from different provenances will differ in their morphological and physiological phenotypes) was supported in that the best model for both growth and resource acquisition variables included provenance as a random effect. For growth variables, the best model (M1) included provenance, but not genotype, as a random effect (based on R^2 and DIC; Table 2). The best model (M9) for resource acquisition variables included both provenance and genotype as random effects (Table 3). Model fit varied across variables and models (Tables 2, 3), and all results presented and discussed are based on models M1 and M9, unless otherwise noted.

Contrary to Hypothesis 1, plants from hotter provenances did not have larger root systems or less aboveground biomass. Yet, one or more provenance random effects were significantly different from zero for all growth variables, except for the root to shoot ratio (Figure 2A). Individuals from provenance 4 (intermediate temperature) generally grew faster (higher average daily growth) and were larger (greater final height, stem diameter, and above-, belowground, and total biomass) than the other provenances. Provenance 2 had less total biomass than the other provenances. Provenance explained more variance in the response variables than either bin or system (Figure 2C) for all growth variables.

One or more provenance random effects were also significant for some resource acquisition variables, but contrary to Hypothesis 1, plants from hotter provenances did not have greater photosynthetic rates or stomatal conductance, lower SLA, or lower TLA. The 95% CI for the provenance 1 random effect did not contain zero for average root diameter, indicating larger roots than the other provenances (Figure 3A). While the 95% CI for all provenances for the other resource acquisition variables overlapped zero, some only marginally overlapped zero (provenance 1 for root length, provenance 2 for photosynthesis and TLA; Figure 3A). While relatively few provenance random effects were individually significant, overall, these random effects generally explained more variation than did bin or system, especially for root length and average root diameter (Figure 3C).

Inundation and initial height effects

Hypothesis 2. (individuals from different provenances will differ in their response to inundation) was not supported. The best model for both growth and resource acquisition variables indicated that the covariate (inundation and initial height) effects do not vary by provenance or genotype (Tables 2, 3). Instead, responses to inundation level or initial height were in the same direction and of similar magnitude for all groups (illustrated in Appendix S1, Figures S4–S6). For growth variables, the positive effect of inundation level indicates that with increasing distance from the water (less inundation), plants grew larger and faster (Figure 2B). Similarly, the positive effect of initial height on many response variables indicates that larger plants at the beginning of the experiment were also larger at the end of the experiment (Figure 2B). Average growth rate, however, was not correlated with initial plant height.

Patterns in covariate effects differed for the resource acquisition variables (Figure 3B) since most variables were not significantly correlated with either inundation level or initial height. Average root diameter, however, was positively correlated with inundation level, meaning average root diameter increased with less inundation. Inundation level and initial height were positively correlated with TLA.

Genotype phenotypic variability and heritability

Hypothesis 3. (phenotypic variation in growth and resources acquisition characteristics and inundation responses will be partially governed by genotype), was partially supported in that the best model (M9) for resource acquisition variables included both provenance and genotype as random effects (Table 3). The SLA values for genotype 6 were significantly larger than other genotypes (Figure 4). All 95% CI for all other genotypes and variables overlapped zero, with the random effect for genotype 9 for photosynthetic rate only marginally overlapping zero. The random effects of genotype generally explained more variation than did bin or system and as much or more than provenance for SLA and TLA (Figure 3C). Results for broad-sense heritability (H^2) also partially supported

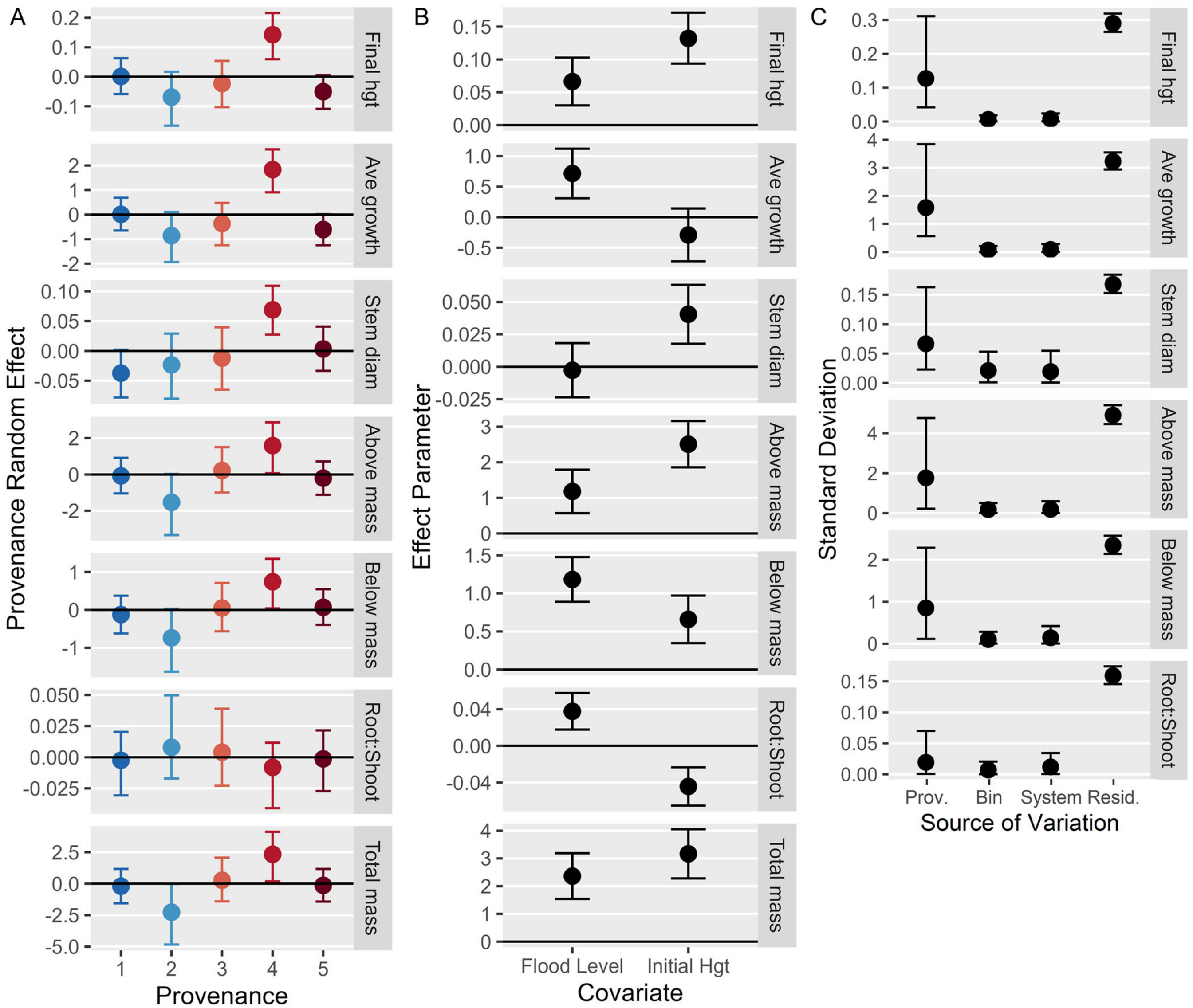

FIGURE 2 Summary of posterior parameter estimates for growth model M1 (see Table 2 for model descriptions). Variables are final height (Final hgt, m), average growth (Ave growth, mm), stem diameter (Stem diam, cm), aboveground biomass (Above mass, g), belowground biomass (Below mass, g), root:shoot ratio (Root:Shoot), and total biomass (Total mass, g). (A) Mean and 95% credible intervals of the provenance random effects. (B) Covariate effects for inundation level and initial height. (C) Variation explained by provenance (Prov.), bin, system, and residual variation (Resid.). Total biomass parameters were calculated from aboveground and belowground biomass values, so variance parameters are not available.

Hypothesis 3 in being significantly greater than zero for SLA: posterior mean and 95% CI for $H^2 = 0.25$ (0.03, 0.55). The 95% CI for H^2 contained zero for the other 11 variables (Appendix S1, Table S7).

DISCUSSION

Differences among provenances

This study indicates that individuals from different provenances exhibit phenotypic differences when the influence of inundation is accounted for, but that differences are not related to the nominal temperature environment of the provenance. In contrast to results from studies on riparian cottonwood trees (e.g., Grady et al., 2013; Cooper et al., 2019; Hultine et al., 2020b), we found that plants from the hottest site (provenance 5) did not exhibit larger root systems, smaller aboveground traits, or lower SLA or TLA than other, cooler provenances. These results indicate that *P. sericea* populations do not exhibit morphological and physiological trends similar to riparian trees and may not have the same adaptive responses to temperature.

Alternative drivers of phenotypic differences across provenances remain unclear. Other provenance environmental conditions may have influenced the phenotypes, such as, but not limited to, flow velocity and erosive

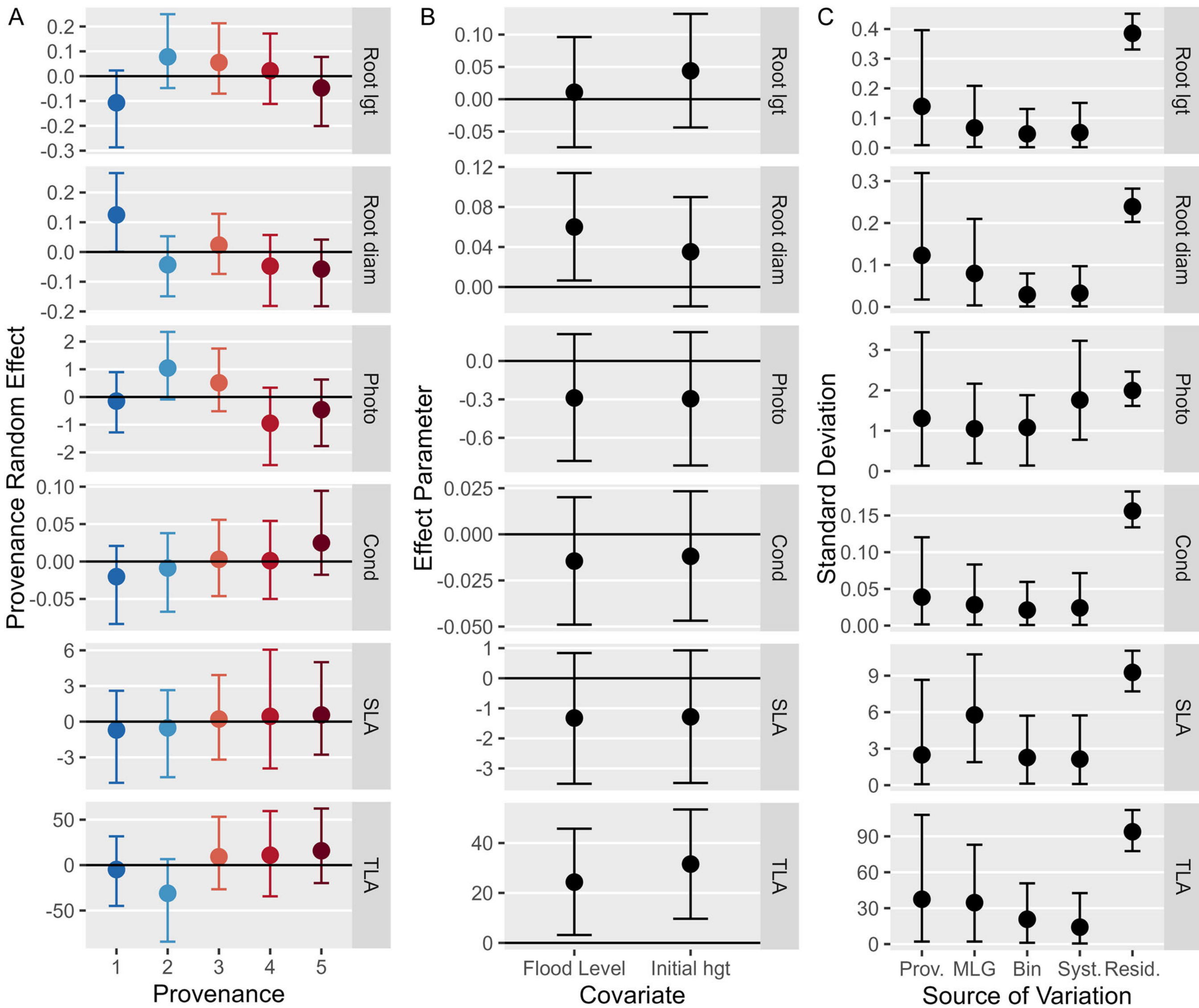

FIGURE 3 Summary of posterior parameter estimates for resource acquisition model M9 (see Table 3 for model descriptions). Variables are root length (Root lgt, log of cm), average root diameter (Root diam, mm), photosynthetic rate (Photo, µmol CO_2 m^{-2} s^{-1}), stomatal conductance (Cond, mol H_2O m^{-2} s^{-1}), specific leaf area (SLA, cm^2 g^{-1}), and total leaf area (TLA, cm^2). (A) Mean and 95% credible intervals of the provenance random effects. (B) Covariate effects for inundation level and initial height. (C) Variation explained by provenance (Prov.), multilocus genotype (MLG), bin, system, residual variation (Resid.).

capacity of flows, which were not quantified in this study. Plants with larger above and belowground structures are expected to be less vulnerable to uprooting in high velocity flow conditions (Bywater-Reyes et al., 2015). The larger root diameter of individuals from the coolest provenance (provenance 1), could be explained by differences in provenance nutrient availability or aerenchyma development. This provenance is nearest to the dam where there is some evidence that dissolved organic carbon and potentially other nutrients are greatest (Ulseth, 2012). Thus, maintaining greater root surface area per unit biomass (i.e., smaller diameter) for nutrient uptake may not be as important at this site. Increases in aerenchyma can increase root diameter (Lambers et al., 2008), but is unlikely here, since increasing root diameter was associated with less inundation.

Alternatively, these provenances could represent a combination of long-existing *P. sericea* stands and newly colonized populations. In this case, phenotypes across provenances could vary due to founder effects in new populations, local adaptation in older populations, and clone age. This species has recently expanded along the Colorado River (Durning et al., 2021), either through new colonization and/or increases through clonal growth. Newly colonized areas could retain the characteristics of the provenance of the source propagules. Clonal expansion of existing populations could retain the characteristics of individuals that predominated before expansion. Patterns in

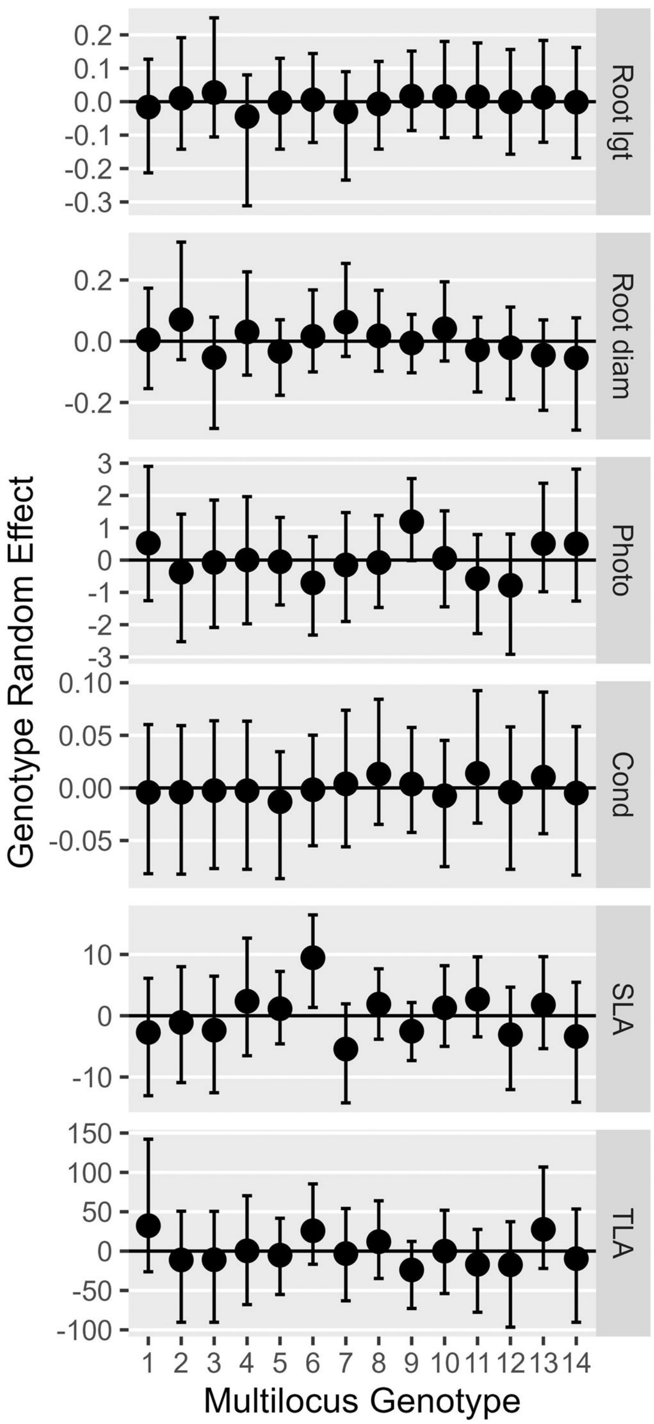

FIGURE 4 Mean and 95% credible intervals for the genotype random effects for resource acquisition variables: root length (Root lgt, log of cm), average root diameter (Root diam, mm), photosynthetic rate (Photo, μmol CO_2 m^{-2} s^{-1}), stomatal conductance (Cond, mol H_2O $m^{-2}s^{-1}$), specific leaf area (SLA, cm^2 g^{-1}), and total leaf area (TLA, cm^2).

phenotypic variability could be the result of a mix of phenotypes from recent colonization and local adaptation.

This study illustrates that differences in growth and morphology may reflect aspects of the complex home ecosystem other than temperature adaptations. For riparian systems, these could be related to a suite of flow characteristics including flow velocity (Bywater-Reyes et al., 2015), sediment deposition and erosion (González et al., 2020; Butterfield et al., 2020b), complex dispersal and colonization patterns (Tabacchi et al., 1998), or human-mediated plant establishment (Smulders et al., 2008; Palmquist et al., 2021). The provenances in this study all span the same shoreline flood gradient, so have likely shared the same flood pattern over time. These populations were also not intentionally manipulated by human activities. Other flow characteristics and plant demographic patterns, then, could account for patterns observed here. A greater understanding of how provenance-specific phenotypic variation relates to a broad suite of environmental characteristics and demographics would be useful for predicting riparian shrub response to environmental change.

Provenances responded similarly to flooding

Despite differences in phenotypes across provenances, Hypothesis 2 was not supported since climatic provenance did not confer unique inundation responses. Root to shoot ratio and SLA, two variables anticipated to result in a trade-off between flooding and heat tolerance, did not differ across provenances, so no difference in response to inundation would be expected. Given the moderate conditions of the greenhouse, it is possible that extreme heat could elicit differences in phenotypes and different inundation responses (Grady et al., 2013; Hultine et al., 2020b).

Growth variables showed different responses to inundation compared to resource acquisition variables. In the inundated conditions, *P. sericea* individuals altered their growth rate, size, root diameter, and TLA rather than leaf-level morphological or gas exchange traits. It may be a common pattern among species that use clonal growth to take advantage of newly available space or resources to have greater variability in root and shoot growth than physiological responses (de Kroons and Hutchings, 1995; Münzbergová et al., 2017).

Decreased root diameter with greater inundation was related to increases in fine roots in this study. Root diameter typically increases with inundation, particularly through the growth and dominance of porous adventitious roots (e.g., Visser et al., 1996; Kozlowski, 1997; Pan et al., 2014). Here, *P. sericea* developed extensive root systems, both from existing roots that extended to the bottom of each tube and from the submerged stem into the water (adventitious roots). The decrease in root diameter under inundated conditions exhibited here may have increased oxygen diffusion to the center of the root (Sauter, 2013).

The role of genotype by environment interactions

Genotype effects contributed to phenotypic characteristics but were not associated with different inundation responses.

Phenotypic characteristics related to growth were more strongly influenced by environment (inundation), whereas those related to resource acquisition were more strongly related to genotype. The relationships between phenotypic plasticity in response to inundation and the heritability of inundation-induced plasticity could have implications for riparian shrubs in changing environments (Laitinen and Nikoloski, 2019; Cooper et al., 2022). Heritability of trait plasticity could translate into rapid phenotypic selection, either improving or reducing a species' likelihood of survival under changing environmental conditions (Laitinen and Nikoloski, 2019; Cooper et al., 2022). The genotypic patterns in this study, based on three loci, represent a minimum level of genetic effect. Development of additional loci could provide greater genotypic resolution and possibly result in stronger genotypic effects and higher or more constrained heritability estimates.

The number of genotypes identified in each provenance decreased with increasing temperature where provenances 4 and 5 (warmest) consist entirely or almost entirely of one genotype (Appendix S1, Table S3). The genotyped individuals from provenance 4 were genetically identical; given the strongly clonal nature of this species, this provenance may consist of one clone that can grow larger and faster than other provenances. *Pluchea sericea* is also more prolific in the downstream portion of the study area, where provenances 4 and 5 occur (Palmquist et al., 2022b). In clonal species that reproduce vigorously and rapidly by rhizomes, a single or a few genotypes can change the genetic landscape and associated ecosystem functions (Saltonstall and Meyerson, 2016). Further research into the genotypic diversity of *P. sericea* in the southwestern United States may be able to identify whether recent regional expansion of this species is related to a few, well-adapted genotypes, changing environmental conditions leading to the species expansion, or a combination of those factors.

CONCLUSIONS

This study indicates that for *P. sericea*, a clonal, riparian shrub, growth is more strongly influenced by inundation rather than genotype, while resource acquisition traits are more closely tied to genotype. The expectation that phenotype would be correlated with the nominal temperature conditions of a provenance is largely inspired by studies on nonclonal, riparian trees, which could explain the different patterns uncovered in this study. Shrubs, and particularly clonal shrubs, seem to differ from trees in their sensitivity to environmental change and the direction of responses (Amlin and Rood, 2001; Grady et al., 2011, 2017). For example, shrubs can exhibit greater sensitivity to abrupt water table decline than trees (Amlin and Rood, 2001), less sensitivity in net primary productivity responses to mean annual temperature changes (Grady et al., 2011), and have complex provenance and genotype responses to interspecific competition (Grady et al., 2017). More studies examining provenance-specific responses of riparian shrubs will be a key part of understanding environmental change impacts on riparian ecosystems. Riparian shrubs can be ecosystem engineers that increase community biodiversity (Bangert et al., 2013) and alter sediment deposition and morphology of river channels (Butterfield et al., 2020b), impacting the template for the rest of the riparian system. In extreme riparian environments—such as alpine, arctic, and desert riparian systems—trees are often absent, making shrubs the dominant overstory plant (Gould and Walker, 1999; Liljedahl et al., 2020). As temperatures and river flows change, the genotype by environment responses of shrubs in riparian systems could have cascading effects on riparian ecosystems.

AUTHOR CONTRIBUTIONS

All authors contributed to ideas and development of the experiment. E.P., B.B., K.O., and T.W. developed the experimental design; E.P., B.B., and G.A. collected data; E.P. and K.O. analyzed the data; E.P., K.O., and B.B. led the writing of the manuscript. All authors contributed to manuscript drafts and gave final approval for publication.

ACKNOWLEDGMENTS

Any use of trade, product, or firm names is for descriptive purposes only and does not imply endorsement by the U.S. Government. Funding was provided by the Glen Canyon Adaptive Management Program, Sigma Xi, Regents' Professor funding to Dr. Thomas Whitham, and Grand Canyon National Park (DUNS #806345542). The authors thank staff of Grand Canyon National Park and Glen Canyon National Recreation Area, Grand Canyon Youth, Cottonwood Group, Ogle Lab, Erica Fraley, Abraham Cadmus, David Ward, Carla Roybal, Ahsa Jensen, Adair Patterson, Andrea Hazelton, Phiyen Nyugen, Hanna Ryder, Clara Krause, Maya Scull, Matt Sommer, Rebecca Best, Hillary Cooper, Lisa Markovchick, Jenny Eckel, Ted Kennedy, Cheyenne Szydlo, Scott Vanderkooi. Thanks to two anonymous reviewers whose suggestions improved this manuscript.

DATA AVAILABILITY STATEMENT

Data generated during this study are available from the USGS ScienceBase-Catalog: https://doi.org/10.5066/P9412RYV (Palmquist et al., 2022a).

ORCID

Emily C. Palmquist http://orcid.org/0000-0003-1069-2154
Kiona Ogle http://orcid.org/0000-0002-0652-8397
Thomas G. Whitham http://orcid.org/0000-0002-1262-4342
Gerard J. Allan http://orcid.org/0000-0002-8007-4784
Patrick B. Shafroth http://orcid.org/0000-0002-6064-871X
Bradley J. Butterfield http://orcid.org/0000-0003-0974-9811

REFERENCES

Amlin, N. A., and S. B. Rood. 2001. Inundation tolerances of riparian willows and cottonwoods. *JAWRA Journal of the American Water Resources Association* 37: 1709-1720.

Arnell, N. W., and S. N. Gosling. 2013. The impacts of climate change on river flow regimes at the global scale. *Journal of Hydrology* 486: 351-364.

Bangert, R., S. M. Ferrier, L. Evans, K. Kennedy, K. C. Grady, E. Hersch-Green, G. J. Allan, and T. G. Whitham. 2013. The proportion of three foundation plant species and their genotypes influence an arthropod community—Restoration implications for the endangered southwestern willow flycatcher. *Restoration Ecology* 21: 447-456.

Blasini, D. E., D. F. Koepke, K. C. Grady, G. J. Allan, C. A. Gehring, T. G. Whitham, S. A. Cushman, and K. R. Hultine. 2021. Adaptive trait syndromes along multiple economic spectra define cold and warm adapted ecotypes in a widely distributed foundation tree species. *Journal of Ecology* 109: 1298-1318.

Blasini, D. E., D. F. Koepke, S. E. Bush, G. J. Allan, C. A. Gehring, T. G. Whitham, T. A. Day, and K. R. Hultine. 2022. Tradeoffs between leaf cooling and hydraulic safety in a dominant arid land riparian tree species. *Plant, Cell & Environment* 45: 1664-1681.

Busch, D. E., and S. D. Smith. 1995. Mechanisms associated with decline of woody species in riparian ecosystems of the southwestern U.S. *Ecological Monographs* 65: 347-370.

Butterfield, B. J., P. E. Grams, L. E. Durning, J. E. Hazel, E. C. Palmquist, B. E. Ralston, and J. B. Sankey. 2020b. Associations between riparian plant morphological guilds and fluvial sediment dynamics along the regulated Colorado River in Grand Canyon. *River Research and Applications* 36: 410-421.

Butterfield, B. J., E. C. Palmquist, and K. R. Hultine. 2020a. Regional coordination between riparian dependence and atmospheric demand in willows (*Salix* L.) of western North America. *Diversity and Distributions* 27: 377-388.

Butterfield, B. J., E. C. Palmquist, and B. E. Ralston. 2018. Hydrological regime and climate interactively shape riparian vegetation composition along the Colorado River, Grand Canyon. *Applied Vegetation Science* 21: 572-583.

Bywater-Reyes, S., A. C. Wilcox, J. C. Stella, and A. F. Lightbody. 2015. Flow and scour constraints on uprooting of pioneer woody seedlings. *Water Resources Research* 51: 9190-9206.

Capon, S. J., L. E. Chambers, R. Mac Nally, R. J. Naiman, P. Davies, N. Marshall, J. Pittock, et al. 2013. Riparian ecosystems in the 21st century: hotspots for climate change adaptation? *Ecosystems* 16: 359-381.

Caster, J. J., T. P. Dealy, T. Andrews, H. Fairley, A. East, and J. B. Sankey. 2014. Meteorological data for selected sites along the Colorado River corridor, Arizona, 2011-13. Open-File Report 2014-1247. U.S. Geological Survey. Reston, VA, USA.

Cooper, H. F., K. C. Grady, J. A. Cowan, R. J. Best, G. J. Allan, and T. G. Whitham. 2019. Genotypic variation in phenological plasticity: Reciprocal common gardens reveal adaptive responses to warmer springs but not to fall frost. *Global Change Biology* 25: 187-200.

Cooper, H. F., R. J. Best, L. V. Andrews, J. P. Corbin, I. Garthwaite, K. C. Grady, C. A. Gehring, et al. 2022. Evidence of climate-driven selection on tree traits and trait plasticity across the climatic range of a riparian foundation species. *Molecular Ecology* 31: 5024-5040.

Curtis, S., I. Goldin, and E. Evangelou. 2015. mcmcplots: Create plots from MCMC output. R package version 0.4.2. Website https://cran.r-project.org/web/packages/mcmcplots/index.html

de Kroons, H., and M. J. Hutchings. 1995. Morphological plasticity in clonal plants: the foraging concept reconsidered. *Journal of Ecology* 83: 143-152.

Durning, L. E., J. B. Sankey, C. B. Yackulic, P. E. Grams, B. J. Butterfield, and T. T. Sankey. 2021. Hydrologic and geomorphic effects on riparian plant species occurrence and encroachment: remote sensing of 360 km of the Colorado River in Grand Canyon. *Ecohydrology* 14: e2344.

Evans, L. M., S. Kaluthota, D. W. Pearce, G. J. Allan, K. Floate, S. B. Rood, and T. G. Whitham. 2016. Bud phenology and growth are subject to divergent selection across a latitudinal gradient in *Populus angustifolia* and impact adaptation across the distributional range and associated arthropods. *Ecology and Evolution* 6: 4565-4581.

González, E., V. Martínez-Fernández, P. B. Shafroth, A. A. Sher, A. L. Henry, V. Garófano-Gómez, and D. Corenblit. 2018. Regeneration of *Salicaceae* riparian forests in the Northern Hemisphere—A new framework and management tool. *Journal of Environmental Management* 218: 374-387.

González, E., P. B. Shafroth, S. R. Lee, S. M. Ostoja, and M. L. Brooks. 2020. Combined effects of biological control of an invasive shrub and fluvial processes on riparian vegetation dynamics. *Biological Invasions* 22: 2339-2356.

Gould, W. A., and M. D. Walker. 1999. Plant communities and landscape diversity along a Canadian Arctic river. *Journal of Vegetation Science* 10: 537-548.

Grady, K. C., S. M. Ferrier, T. E. Kolb, S. C. Hart, G. J. Allan, and T. G. Whitham. 2011. Genetic variation in productivity of foundation riparian species at the edge of their distribution: implications for restoration and assisted migration in a warming climate. *Global Change Biology* 17: 3724-3735.

Grady, K. C., D. C. Laughlin, S. M. Ferrier, T. E. Kolb, S. C. Hart, G. J. Allan, and T. G. Whitham. 2013. Conservative leaf economic traits correlate with fast growth of genotypes of a foundation riparian species near the thermal maximum extent of its geographic range. *Functional Ecology* 27: 428-438.

Grady, K. C., T. E. Wood, T. E. Kolb, E. I. Hersch-Green, S. M. Shuster, C. A. Gehring, S. C. Hart, et al. 2017. Local biotic adaptation of trees and shrubs to plant neighbors. *Oikos* 126: 583-593.

Grill, G., B. Lehner, A. E. Lumsdon, G. K. MacDonald, C. Zarfl, and C. R. Liermann. 2015. An index-based framework for assessing patterns and trends in river fragmentation and flow regulation by global dams at multiple scales. *Environmental Research Letters* 10: 015001.

Hultine, K. R., G. J. Allan, D. Blasini, H. M. Bothwell, A. Cadmus, H. F. Cooper, C. E. Doughty, et al. 2020b. Adaptive capacity in the foundation tree species *Populus fremontii*: implications for resilience to climate change and non-native species invasion in the American Southwest. *Conservation Physiology* 8: coaa061.

Hultine, K. R., R. Froend, D. Blasini, S. E. Bush, M. Karlinski, and D. F. Koepke. 2020a. Hydraulic traits that buffer deep-rooted plants from changes in hydrology and climate. *Hydrological Processes* 34: 209-222.

Ikeda, D. H., T. L. Max, G. J. Allan, M. K. Lau, S. M. Shuster, and T. G. Whitham. 2017. Genetically informed ecological niche models improve climate change predictions. *Global Change Biology* 23: 164-176.

Jeplawy, J. R., H. F. Cooper, J. Marks, R. L. Lindroth, M. I. Andrews, Z. G. Compson, C. Gehring, et al. 2021. Plastic responses to hot temperatures homogenize riparian leaf litter, speed decomposition, and reduce detritivores. *Ecology* 102: e03461.

Kamvar, Z. N., J. F. Tabima, and N. J. Grünwald. 2014. *Poppr*: an R package for genetic analysis of populations with clonal, partially clonal, and/or sexual reproduction. *PeerJ* 2: e281.

Kozlowski, T. T. 1997. Responses of woody plants to flooding and salinity. *Tree Physiology Monograph No. 1* 17: 1-29.

Kozlowski, T. T. 2002. Physiological-ecological impacts of flooding on riparian forest ecosystems. *Wetlands* 22: 550-561.

Laitinen, R. A. E., and Z. Nikoloski. 2019. Genetic basis of plasticity in plants. *Journal of Experimental Botany* 70: 739-745.

Lambers, H., F. S. Chapin, and T. L. Pons. 2008. Plant physiological ecology. Springer, NY, NY, USA.

Liljedahl, A. K., I. Timling, G. V. Frost, and R. P. Daanen. 2020. Arctic riparian shrub expansion indicates a shift from streams gaining water to those that lose flow. *Communications Earth & Environment* 1: 50.

Lindborg, R., M. Ermold, L. Kuglerová, R. Jansson, K. W. Larson, A. Milbau, and S. A. Cousins. 2021. How does a wetland plant respond to increasing temperature along a latitudinal gradient? *Ecology and Evolution* 11: 16228-16238.

Long, R. W., S. E. Bush, K. C. Grady, D. R. Smith, D. L. Potts, C. M. D'Antonio, T. L. Dudley, et al. 2017. Can local adaptation explain varying patterns of herbivory tolerance in a recently introduced woody plant in North America? *Conservation Physiology* 5: cox016.

Loreti, J., and M. Oesterheld. 1996. Intraspecific variation in the resistance to flooding and drought in populations of *Paspalum dilatatum* from different topographic positions. *Oecologia* 108: 279-284.

Maurer, E. P., G. Kayser, L. Doyle, and A. W. Wood. 2018. Adjusting flood peak frequency changes to account for climate change impacts in the western United States. *Journal of Water Resources Planning and Management* 144: 05017025.

Mayjonade, B., J. Gouzy, C. Donnadieu, N. Pouilly, W. Marande, C. Callot, N. Langlade, and S. Muños. 2016. Extraction of high-molecular-weight genomic DNA for long-read sequencing of single molecules. *Biotechniques* 61: 203-205.

Moran, E. V., F. Hartig, and D. M. Bell. 2016. Intraspecific trait variation across scales: implications for understanding global change responses. *Global Change Biology* 22: 137-150.

Münzbergová, Z., V. Hadincová, H. Skálová, and V. Vandvik. 2017. Genetic differentiation and plasticity interact along temperature and precipitation gradients to determine plant performance under climate change. *Journal of Ecology* 105: 1358-1373.

Musselman, K. N., F. Lehner, K. Ikeda, M. P. Clark, A. F. Prein, C. Liu, M. Barlage, and R. Rasmussen. 2018. Projected increases and shifts in rain-on-snow flood risk over western North America. *Nature Climate Change* 8: 808-812.

Nicotra, A. B., O. K. Atkin, S. P. Bonser, A. M. Davidson, E. J. Finnegan, U. Mathesius, P. Poot, et al. 2010. Plant phenotypic plasticity in a changing climate. *Trends in Plant Science* 15: 684-692.

Nilsson, C., C. A. Reidy, M. Dynesius, and C. Revenga. 2005. Fragmentation and flow regulation of the world's large river systems. *Science* 308: 405-408.

Ogle, K., and J. J. Barber. 2020. Ensuring identifiability in hierarchical mixed effects Bayesian models. *Ecological Applications* 30: e02159.

Palmquist, E. C., G. J. Allan, K. Ogle, T. G. Whitham, B. J. Butterfield, and P. B. Shafroth. 2021. Riverine complexity and life history inform restoration in riparian environments in the southwestern U.S. *Restoration Ecology* 29: e13418.

Palmquist, E. C., B. J. Butterfield, and G. J. Allan. 2022a. Arrowweed (*Pluchea sericea*) morphological and physiological response data from a greenhouse inundation experiment: U.S. Geological Survey data release.

Palmquist, E. C., B. J. Butterfield, and B. E. Ralston. 2022b. Five-year status and trends of riparian vegetation in Glen and Grand Canyons downstream of Glen Canyon Dam. Open-File Report, U.S. Geological Survey, Reston, VA, USA. https://doi.org/10.5066/P9KEHY2S

Pan, Y., Y. H. Xie, Z. M. Deng, Y. Tang, and D. D. Pan. 2014. High water level impedes the adaptation of *Polygonum hydropiper* to deep burial: responses of biomass allocation and root morphology. *Scientific Reports* 4: 5612.

Perry, L. G., D. C. Andersen, L. V. Reynolds, S. M. Nelson, and P. B. Shafroth. 2012. Vulnerability of riparian ecosystems to elevated CO_2 and climate change in arid and semiarid western North America. *Global Change Biology* 18: 821-842.

Plummer, M. 2003. JAGS: A program for analysis of bayesian graphical models using Gibbs sampling. *In* K. Hornik and A. Zeileis [eds.], Proceedings of the 3rd International Workshop on Distributed Statistical Computing (DSC 2003), Vienna, Austria, 1-10.

Plummer, M., N. Best, K. Cowles, and K. Vines. 2006. CODA: convergence diagnosis and output analysis for MCMC. *R News* 6: 7-11.

Plummer, M., A. Stukalov, M. Denwood, and M. M. Plummer. 2019. Package 'rjags'. Website https://cran.r-project.org/web/packages/rjags/index.html.

Poff, N. L., J. D. Olden, D. M. Merritt, and D. M. Pepin. 2007. Homogenization of regional river dynamics by dams and global biodiversity implications. *Proceedings of the National Academy of Sciences, USA* 104: 5732-5737.

R Core Team. 2014. A language and environment for statistical computing. R Foundation for Statistical Computing, Vienna, Austria. Website https://www.R-project.org.

Reents, S., P. Mueller, H. Tang, K. Jensen, and S. Nolte. 2021. Plant genotype determines biomass response to flooding frequency in tidal wetlands. *Biogeosciences* 18: 403-411.

Rodríguez, M. E., D. Lauff, S. Cortizo, and V. M. C. Luquez. 2019. Variability in flooding tolerance, growth and leaf traits in a *Populus deltoides* intraspecific progeny. *Tree Physiology* 40: 19-29.

Saltonstall, K., and L. A. Meyerson. 2016. *Phragmites australis*: from genes to ecosystems. *Biological Invasions* 18: 2415-2420.

Sauter, M. 2013. Root responses to flooding. *Current Opinion in Plant Biology* 16: 282-286.

Smulders, M. J. M., J. E. Cottrell, F. Lefèvre, J. van der Schoot, P. Arens, B. Vosman, H. E. Tabbener, et al. 2008. Structure of the genetic diversity in black poplar (*Populus nigra* L.) populations across European river systems: consequences for conservation and restoration. *Forest Ecology and Management* 255: 1388-1399.

Tabacchi, E., D. L. Correll, R. Hauer, G. Pinay, A.-M. Planty-Tabacchi, and R. C. Wissmar. 1998. Development, maintenance and role of riparian vegetation in the river landscape. *Freshwater Biology* 40: 497-516.

Topping, D. J., J. C. Schmidt, and L. E. Vierra. 2003. Computation and analysis of the instantaneous-discharge record for the Colorado River at Lees Ferry, Arizona—May 8, 1921, through September 30, 2000. Professional Paper 1677, U.S. Geological Survey, Reston, VA, USA.

Turner, R. M., and M. M. Karpiscak. 1980. Recent vegetation changes along the Colorado River between Glen Canyon Dam and Lake Mead, Arizona. Professional Paper 1132, U.S. Geological Survey, Reston, VA, USA.

Ulseth, A. J. 2012. Sources, fates, and export of organic carbon in the Colorado River Basin. Ph.D. dissertation, University of Wyoming, Laramie, WY, USA.

Vandersande, M. W., E. P. Glenn, and J. L. Walworth. 2001. Tolerance of five riparian plants from the lower Colorado River to salinity drought and inundation. *Journal of Arid Environments* 49: 147-159.

Visser, E., C. Blom, and L. Voesenek. 1996. Flooding-induced adventitious rooting in *Rumex*: morphology and development in an ecological perspective. *Acta Botanica Neerlandica* 45: 17-28.

Westerband, A. C., J. L. Funk, and K. E. Barton. 2021. Intraspecific trait variation in plants: a renewed focus on its role in ecological processes. *Annals of Botany* 127: 397-410.

Whitham, T. G., C. A. Gehring, L. J. Lamit, T. Wojtowicz, L. M. Evans, A. R. Keith, and D. S. Smith. 2012. Community specificity—Life and afterlife effects of genes. *Trends in Plant Science* 17: 271-281.

Whitlock, M. C. 2008. Evolutionary inference from QST. *Molecular Ecology* 17: 1885-1896.

Wright, A. J., H. de Kroon, E. J. W. Visser, T. Buchmann, A. Ebeling, N. Eisenhauer, C. Fischer, et al. 2017. Plants are less negatively affected by flooding when growing in species-rich plant communities. *New Phytologist* 213: 645-656.

Yang, Y., S. Huang, Y. Wang, L. Gui, Y. Liu, X. Huang, G. Chen, et al. 2018. Development of EST-SSR markers for *Pluchea indica* (Asteraceae) and cross-amplification in related species. *Applications in Plant Sciences* 6: e01173.

SUPPORTING INFORMATION

Additional supporting information can be found online in the Supporting Information section at the end of this article.

Appendix S1. Additional information on collection locations, experimental design, plant measurements, summary statistics, genotypes, variable correlations, and model specifications, including Tables S1–S7 and Figures S1–S5.

How to cite this article: Palmquist, E. C., K. Ogle, T. G. Whitham, G. J. Allan, P. B. Shafroth, and B. J. Butterfield. 2023. Provenance, genotype, and flooding influence growth and resource acquisition characteristics in a clonal, riparian shrub. *American Journal of Botany* 110(2): e16115. https://doi.org/10.1002/ajb2.16115